GSDME maintains hematopoietic stem cells by balancing pyroptosis and apoptosis

Xiuxiu Yang, Tingting Cong, Hanqing He, Jianwei Wang*

School of Pharmaceutical Sciences, Tsinghua University, Beijing 100084, China

Abstract

GSDME contains a pore-forming domain at its N-terminal region to execute pyroptosis. Our previous study has reported that forced expression of *Gsdme* impairs the reconstitution capacity of hematopoietic stem cells (HSCs). While, how GSDME-mediated pyroptosis regulates HSCs remains unknown. Here, we show that hematopoietic stem and progenitor cells are capable to undergo pyroptosis in response to cisplatin treatment and GSDME is one of the genes mediating such process. *Gsdme*$^{-/-}$ mice revealed no difference in the steady state of blood system while *Gsdme*$^{-/-}$ HSCs exhibited compromised reconstitution capacity due to increased apoptosis. Briefly, this study reveals that GSDME modulates HSC function by coordinating pyroptosis and apoptosis.

Keywords: Apoptosis, GSDME, Hematopoietic stem cell, Programmed cell death, Pyroptosis

1. INTRODUCTION

Hematopoietic stem cells (HSCs) are the source of all the blood cells. Based on their self-renewal and differentiation ability, HSCs maintain the life-long homeostasis of the blood system. Accumulating evidences have suggested that programmed cell death (PCD) plays an essential role in HSC maintenance.[1–5] Apoptosis, necroptosis, and pyroptosis are the most intensively investigated PCD forms in recent years.[6–8] Inhibition of HSCs' apoptosis enhances their repopulation potential or resistance to lethal challenges.[1,2,9] Meanwhile, several studies have shown that apoptosis serves to clear senescent or damaged HSCs.[3,10] In addition to apoptosis, necroptosis is a form of programmed necrosis,[6] which is triggered by TNF super-families and executed by the pore-forming protein MLKL.[11,12] It has been reported that necroptosis is involved in HSC death or reconstitution defects.[4,13] In addition to mediating cell death, PCD-related genes perform other functions in HSCs. For example, the apoptosis executor Caspase-3 and the phosphorylated form of pro-apoptotic protein BID maintain the quiescence of HSCs by regulating responsiveness to environmental cytokines or oxidative stress respectively.[14,15]

Pyroptosis is another type of programmed necrotic cell death and is executed by gasdermin family proteins, including GSDMA, GSDMB, GSDMC, GSDMD, and GSDME.[16] Pyroptotic cell death has caused lots of concerns in recent years,[17–19] while its role in HSCs remains poorly understood. One study has ever reported that the activating mutation of NLRP1a, which is a scaffold of the inflammasome,[20] drives hematopoietic progenitor cells depletion via Caspase-1 dependent pyroptosis,[5] wherein GSDMD plays a key role.[20] GSDME-mediated pyroptosis is activated by caspase-3 or killer cell-derived Granzyme B. The high expression of GSDME in hematopoietic and stem cells (HSPCs)[21] implies that GSDME may play an essential role in HSC maintenance, while how GSDME modulates HSC function remains unknown.

Our previous work has found that forced expression of *Gsdme* impairs the reconstitution capacity of HSCs.[21] In this study, we employed *Gsdme*$^{-/-}$ mice to investigate the function of GSDME in HSC maintenance and we observed that GSDME has no significant effect on steady-state hematopoiesis. However, *Gsdme*$^{-/-}$ HSCs displayed compromised reconstitution capacity due to increased apoptotic activity. Moreover, pyroptosis happens in cisplatin-treated HSPCs, wherein GSDME is one of the mediators. In brief, this study reveals the important role of GSDME in HSC maintenance.

* *Address correspondence: Jianwei Wang, PhD, School of Pharmaceutical Sciences, Tsinghua University, Beijing 100084, China.*
E-mail address: jianweiwang@mail.tsinghua.edu.cn (J.W. Wang).

The authors declare no conflicts of interest.

This work was supported by grant numbers 2018YFA0800200, 2017YFA0104000, Z181100001818005 to J.W.W. from the National Key R&D Program of China or the Beijing Municipal Science & Technology Commission.

Author contributions: Conceptualization, J.W.W.; Methodology, X.X.Y.; Investigation, X.X.Y., T.T.C., and H.Q.H.; Writing - original draft, J.W.W.; Writing - review and editing, J.W.W.; Funding Acquisition, J.W.W.; Supervision, J.W.W.

Blood Science, (2021) 3, 40-47

Received August 4, 2020; Accepted October 19, 2020.

http://dx.doi.org/10.1097/BS9.0000000000000064

2. RESULTS

2.1. GSDME is dispensable for the homeostasis maintenance of blood system

To clarify whether the deletion of *Gsdme* affects the steady state maintenance of the blood system, we performed the complete blood cell count. The results revealed that the numbers of red blood cells, white blood cells, neutrophils, lymphocytes, and platelets hold static (Fig. 1A). Next, we analyzed the lineage distribution in peripheral blood (PB) and bone marrow (BM) of *Gsdme*$^{-/-}$ mice and WT littermates. We observed no difference in the percentage of T cells, B cells, and myeloid cells between *Gsdme*$^{-/-}$ and WT mice (Fig. 1B, C). We then investigated the HSCs and progenitors of *Gsdme*$^{-/-}$ mice and observed that both the percentage and the total cell number of LT-HSCs (long-term HSCs), ST-HSCs (short-term HSCs), LSKs (Lin$^-$/Sca-1$^+$/c-Kit$^+$), MPPs (multipotent progenitor), CLPs (common lymphoid progenitors), GMPs

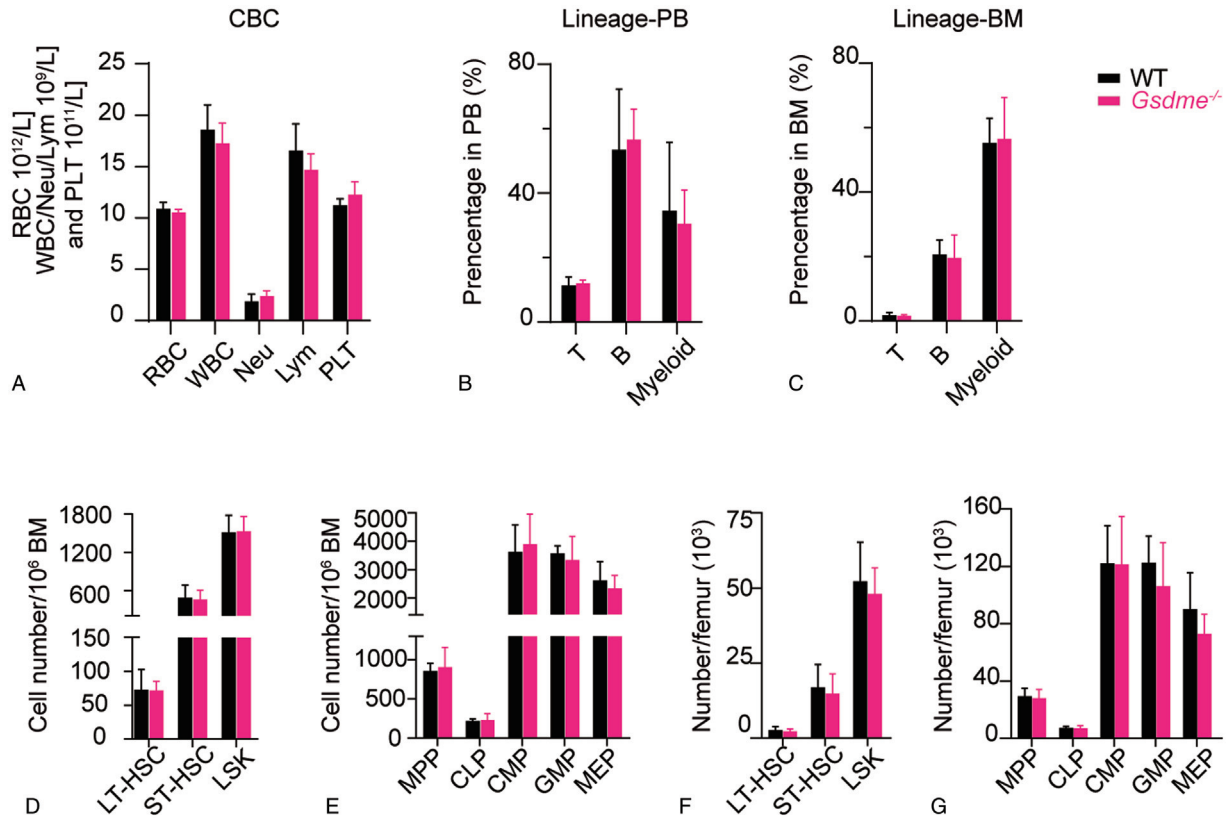

Figure 1. GSDME is dispensable for the homeostasis maintenance of blood system. (A) The histogram exhibits the complete blood cell counts (CBC) of peripheral blood (PB) from WT or *Gsdme*$^{-/-}$ mice, including RBC (red blood cell), WBC (white blood cell), Neu (neutrophil), Lym (lymphocyte) and PLT (platelet). Data are shown as mean ± SD, n = 14 mice for WT and 9 mice for *Gsdme*$^{-/-}$ group. (B, C) This histogram shows the lineage distribution of PB (B) and bone marrow (BM) (C) for WT and *Gsdme*$^{-/-}$ mice, including T cells (CD3$^+$), B cells (B220$^+$), and myeloid cells (CD11b$^+$). Data are shown as mean ± SD, n = 6 mice for WT and 4 mice for *Gsdme*$^{-/-}$ group. (D–G)The histograms display the frequency (D, E) and absolute number (F, G) of HSPCs in the femur of WT and *Gsdme*$^{-/-}$ mice, including LT-HSC (long term-HSC, CD34$^-$/Flt3$^-$LSK), ST-HSC (short term-HSC, CD34$^+$/Flt3$^-$LSK), LSK (Lin$^-$/Sca1$^+$/c-Kit$^+$) (D, F), MPP (multipotent progenitor, CD34$^+$/Flt3$^+$/LSK), CLP (common lymphoid progenitor, CD127$^+$/Flt3$^+$/LS^{low}K^{low}), CMP (common myeloid progenitor, Lin$^-$/Sca1$^-$/c-Kit$^+$/CD34$^+$/CD16/32^{low}), GMP (granulocyte/macrophage progenitor, Lin$^-$/c-Kit$^+$/Sca1$^-$/CD34$^+$/CD16/32^{high}) and MEP (megakaryocytic/erythroid progenitor, Lin$^-$/c-Kit$^+$/Sca1$^-$/CD34$^-$/CD16/32$^-$) (E, G). Data are shown as mean ± SD, n = 6 mice for WT and 4 mice for *Gsdme*$^{-/-}$ group. Adult mice of 2- to 3-month old were analyzed for (A-G).

(granulocyte/macrophage progenitors) and MEPs (megakaryocytic/erythroid progenitors) hold static in *Gsdme*$^{-/-}$ mice compared to WT littermates (Fig. 1**D–G**). In summary, GSDME has almost no effect on the steady-state maintenance of the blood system.

2.2. GSDME is indispensable for HSCs rebuilding blood system

To evaluate the impact of *Gsdme* deficiency on the long-term hematopoietic reconstitution capacity of HSCs, we performed the competitive HSC transplantation assay. 50 HSCs were freshly isolated from either *Gsdme*$^{-/-}$ mice or WT literates and co-transplanted with competitor cells into lethally irradiated congenic recipients (Fig. 2**A**). The chimerism in the PB was evaluated every month post HSC transplantation (HSCT) until the fourth month (Sup. Fig. 1A and B, http://links.lww.com/BS/A26). The result showed that *Gsdme*$^{-/-}$ HSCs displayed significantly impaired reconstitution capacity, with reduced overall, T-lymphoid, and B-lymphoid chimerism (Fig. 2**B**). The lineage distribution of donor-derived PB cells by the end of the fourth month post HSC transplantation revealed no difference between *Gsdme*$^{-/-}$ and WT HSCs (Fig. 2**C**). Furthermore, we analyzed hematopoietic stem and progenitor cells of recipients to evaluate the engraftment rate of donor-derived HSCs and LSKs. We observed no significant difference of HSCs between *Gsdme*$^{-/-}$ and WT group (Fig. 2**D**), but slightly reduced LSK cells in *Gsdme*$^{-/-}$ group (Fig. 2**D**), indicating that GSDME might play a role in hematopoietic progenitor cells proliferation, but not HSCs.

To further confirm that the loss of function of *Gsdme* impairs HSC reconstitution capacity, we conducted an RNAi experiment on transplanted HSCs with shRNA targeting GSDME. The shRNA showed a good knockdown efficiency at the protein level (Fig. 2**E**, shRNA sequence was shown in the Section 4). Virally transduced LSKs were isolated at day 3 post the lentivirus infection and then transplanted into recipient mice with competitor cells, PB chimerism was evaluated every month until the third month (Fig. 2**F**). The result showed that the knockdown of GSDME severely impaired the long-term reconstitution capacity of HSCs, with reduced overall, lymphoid, and myeloid reconstitution (Fig. 2**G**). Moreover, HSCs caring GSDME shRNA displayed increased differentiation skewing toward T and B lymphocytes but reduced myeloid differentiation by the end of the third month (Fig. 2**H**). Given that the knockdown of *Gsdme* had a more severe effect than the knockout of *Gsdme* on the reconstitution capacity of HSCs (Fig. 2**B, G**). The possible explanation is that a genetic compensation response may occur in *Gsdme*$^{-/-}$ HSCs, since the nonsense codons generated by truncated mutations can upregulate the transcription of related compensation genes.[22] Taken together, these results suggest that GSDME is essential for HSC reconstitution.

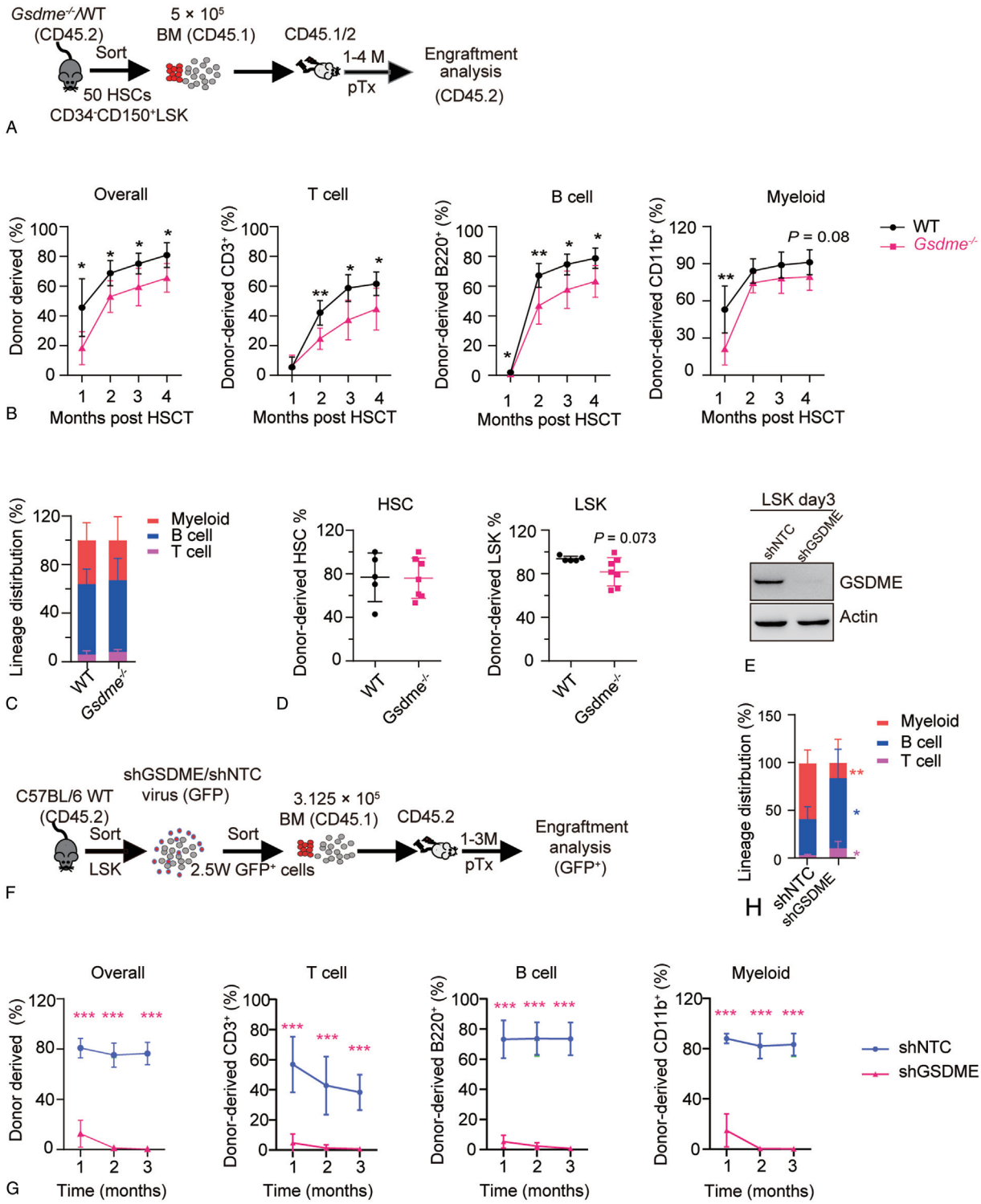

Figure 2. *Gsdme* deficiency deteriorates the reconstitution ability of HSCs. (A-C) Freshly isolated 50 HSCs from WT or *Gsdme*$^{-/-}$ mice were transplanted into lethally irradiated recipients together with 5×10^5 competitor cells. Chimerism in PB was evaluated every month until the fourth month post transplantation (Tx). (A) The schematic diagram showing the experimental design for HSC competitive transplantation. (B) The line plots showing donor chimerism in overall (CD45.2$^+$), T (CD3$^+$), B (B220$^+$) and myeloid (CD11b$^+$) cells every month after HSC transplantation (HSCT) (n = 5 for WT and 7 for *Gsdme*$^{-/-}$ group). (C) This histogram displays the lineage distribution of donor-derived PB at the fourth month after transplantation (n = 5 for WT and 7 for *Gsdme*$^{-/-}$ group). Data are shown as mean ± SD. (D) These scatter plots depict donor-derived HSC (left) and LSK (right) engraftment in recipient BM by the end of the fourth month post HSC transplantation (n = 5 for WT and 7 for *Gsdme*$^{-/-}$ group). Data are shown as mean ± SD. The gating strategy for donor chimerism and lineage distribution is in Sup. Fig. 1A and B, http://links.lww.com/BS/A26. (E) Representative Western blot showing knockdown efficiency of GSDME in LSKs. Freshly isolated 10^5 LSKs were infected with the shRNA targeting GSDME or the none target control (NTC) vector for 3 days. The whole cell lysates were subjected to Western blot using the antibody against GSDME. (F–H) 25,000 GFP$^+$ cells were isolated from GSDME-shRNA or shNTC (the non-target control shRNA) transduced LSKs at day3 post infection and transplanted into lethally irradiated recipients together with 3.125×10^5 competitor cells. Chimera in PB was evaluated every month until the third month. (F) The schematic diagram showing the experimental design for the transplantation of GSDME-shRNA transduced LSKs. (G) The line plots depict changes in PB chimerism of donor-derived cells (GFP$^+$) in recipients at the indicated time

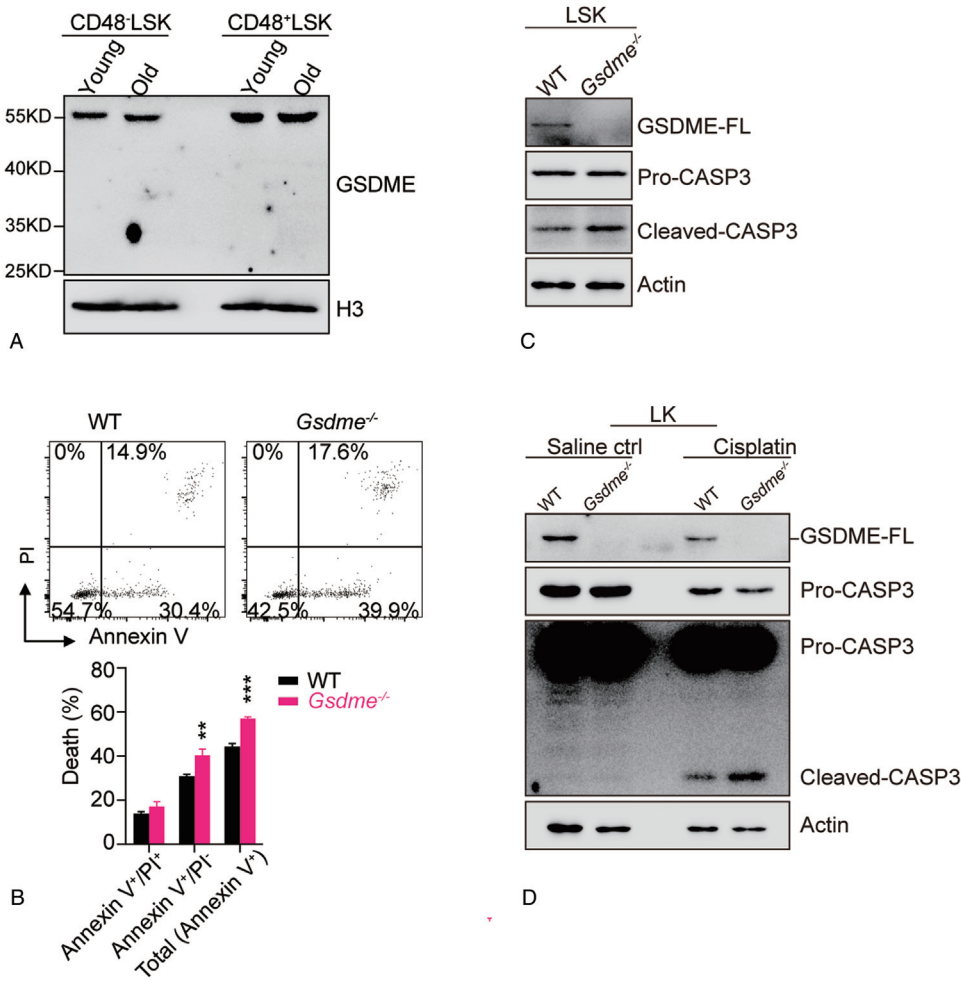

Figure 3. *Gsdme* deficiency augments the apoptotic activity and apoptotic sensitivity of proliferative HSCs. (A) Representative Western blot showing the expression of GSDME in HSPCs from young and old mice. 20,000 freshly isolated HSCs ($CD48^-LSK$) and HPCs ($CD48^+LSK$) were subjected to Western blot using indicated antibodies. (B) Representative flow cytometry plots (top) and histograms (bottom) showing cell viability of LSKs from WT and $Gsdme^{-/-}$ mice. Freshly isolated LSKs were cultured for 24 h before the cell viability analysis by Annexin-V and PI staining. n = 3 technical repeats per group, data are shown as mean ± SD. (C and D) Representative Western blot showing the activity of Caspase-3 in the LSKs (C) and LKs (D) from WT and $Gsdme^{-/-}$ mice. Cell lysates were subjected to Western blot using indicated antibodies. Fresh isolated LSKs in (C) were cultured for 24 h and the LKs in (D) were cultured overnight and treated with 40 μg/ml cisplatin for 5 h before the Western blot assay.

2.3. *Gsdme* deficiency augments the apoptotic activity and apoptotic sensitivity of proliferative HSCs

Given that both forced or inadequate expression of GSDME impairs the long-term reconstitution potential of HSCs, and that the reconstitution ability of HSCs declines in aged mice,[23] we wonder whether GSDME correlates with HSC aging. To address this question, we performed Western blot on HSCs ($CD48^-LSK$) and HPCs ($CD48^+LSK$) from aged (28 months) and young mice (3 months). The result showed that neither the expression nor activity of GSDME was changed in the aged hematopoietic system (Fig. 3A). Activated GSDME, the N-terminal GSDME,[24] is not detectable in HSCs or HPCs of both aged and young mice (Fig. 3A). Thus, GSDME-mediated pyroptosis may not play a role in HSC aging.

Next, we aimed to investigate the role of GSDME in maintaining HSC viability. By Annexin-V binding and Propidium iodide (PI) uptake, we can distinguish and quantify apoptotic and necrotic cells.[25] 8000 LSKs isolated from WT and $Gsdme^{-/-}$ mice were seeded and analyzed 24 hours later. The data showed that the frequency of total dead ($Annexin\text{-}V^+$) cells and apoptotic cells ($Annexin\text{-}V^+/PI^-$) increased in $Gsdme^{-/-}$ LSKs (Fig. 3B), indicating that cell viability of *Gsdme*-deficient HSPCs decreases upon proliferation. Given that activated Caspase-3 (cleaved-CASP3) is considered as the hallmark of apoptosis,[26] we then sought to evaluate the activation of Caspase-3 in $Gsdme^{-/-}$ LSKs after 24 hours of cultivation. The result showed that cleaved-CASP3 was elevated in $Gsdme^{-/-}$ LSKs (Fig. 3C), which confirms the higher apoptotic activity of *Gsdme*-deficient HSPCs upon proliferation.

points after transplantation. (H) This histogram displays the lineage distribution of donor-derived PB by the end of the third month after transplantation. The recipients with an overall donor chimerism higher than 0.1% were analyzed in (H). Data are shown as mean ± SD, n = 8 mice for shNTC (G and H), 7 mice for shGSDME (G), and 6 mice for shGSDME (H).

We then set ought to evaluate the apoptotic sensitivity of *Gsdme*-deficient hematopoietic progenitor cells in response to apoptotic stimuli. We treated *Gsdme*$^{-/-}$ LK (Lin$^-$/Sca-1$^-$/c-Kit$^+$) cells with cisplatin, which is a well-known drug to induce mitochondrial apoptosis by generating DNA lesions.[27] We observed the activation of Caspase-3 in WT LK cells upon cisplatin treatment, while more Caspase-3 was activated in *Gsdme*$^{-/-}$ LK cells (Fig. 3**D**), indicating that the apoptotic sensitivity is increased in *Gsdme*$^{-/-}$ hematopoietic progenitor cells.

2.4. GSDME is involved in cisplatin-induced pyroptosis in HSPCs

Cisplatin has been reported to induce pyroptosis in some GSDME-expressing cancer cells.[24] Given the expression of GSDME in HSCs and progenitor cells (Fig. 3**A**), we sought out to investigate whether GSDME-mediated pytoptosis happens in HSPCs. We treated WT LSK cells with cisplatin and examined the morphology of cell death by bright-field images. The result showed that cisplatin-treated LSK cells exhibited the morphology of pyroptosis, which is characterized by cell swelling and large bubbles from the plasma membrane (Fig. 4**A**).[24] The cell viability result showed that WT LSKs shifted to Annexin-V$^+$/PI$^+$ upon cisplatin treatment (Fig. 4**B**), indicating that pyroptosis may be a form of LSK cell death. Given that the N-terminus of GSDME (GSDME-N) was responsible for the execution of GSDME-dependent pyroptosis, we then evaluated GSDME and found that GSDME-N was produced in LSKs upon cisplatin treatment (Fig. 4**C**). Taken together, these data imply that cisplatin-treated LSKs undergo GSDME-mediated pyroptosis. Next, we sought out to evaluate whether GSDME is the only mediator in this process, we then treated LSKs from WT and *Gsdme*$^{-/-}$ mice with cisplatin for 6 hours and subsequently evaluated the percentage of pyroptotic cells indicated by the black arrow in the image (Fig. 4**D**). We observed that the percentage of pyroptotic cells in the WT group increased to 30% upon cisplatin treatment, while it was 22% in *Gsdme*$^{-/-}$ group, which is significantly decreased than the WT group (Fig. 4**E**), indicating that GSDME does participate in cisplatin-induced pyroptosis in HSPCs. However, the pyroptotic morphology still existed in *Gsdme*$^{-/-}$ LSK cells (Fig. 4**D**), suggesting that GSDME is not the only mediator of cisplatin-induced cell death in HSPCs. The involvement of GSDME in cisplatin-induced pyroptosis was further confirmed by the reduced PI uptake in *Gsdme*$^{-/-}$ LSK cells (Fig. 4**F**).

Cisplatin-treated LK cells also presented extensive pyroptotic morphology and the production of N-terminal GSDME (Fig. 4**G, H**), and only an increase of necrotic cell death can be detected for WT LKs by Annexin-V and PI analysis (Fig. 4**I,J**). The pyroptotic morphology was further confirmed by the chemotherapy drug doxorubicin and etoposide (Sup. Fig. S2, http://links.lww.com/BS/A26), both of which were confirmed to induce GSDME-mediated pyroptosis in GSDME-expressing tumor cells.[24] Given the higher activity of Caspase-3 induced in *Gsdme*$^{-/-}$ LKs (Fig. 3**D**), it is important to investigate the influence of *Gseme* deficiency on cell death of HPCs in response to cisplatin. To address this question, we performed the cell viability assay using *Gsdme*$^{-/-}$ LKs (Fig. 4**I**) and observed that *Gsdme*$^{-/-}$ LKs displayed reduced necrosis (Annexin-V$^+$/PI$^+$, Fig. 4**J**-left) and increased apoptosis (Annexin-V$^+$/PI$^-$, Fig. 4**J**-middle) after cisplatin treatment, but their viability was still lower than that of WT LKs according to the higher frequency of Annexin-V$^+$ cells for *Gsdme*$^{-/-}$ LKs (Fig. 4**J**-right). Moreover, *Gsdme*$^{-/-}$ LKs slightly enhanced the apoptotic cell death but did not switch to apoptosis after cisplatin treatment (Annexin-V$^+$/PI$^-$, Fig. 4**J**-middle). The results suggest that GSDME plays a role in leading to cisplatin-induced necrotic cell death in HPCs but seems to have little effect on cisplatin-induced cell viability loss, and that other forms of necrosis play a dominant role in leading to the death of *Gsdme*$^{-/-}$ HPCs after cisplatin treatment instead of apoptosis.

3. DISCUSSION

Caspase-3 activation in HSCs has long been considered a hallmark of apoptosis. Here, we provide evidence that the activation of Caspase-3 in HSCs induced by cisplatin is able to lead to GSDME-mediated pyroptosis. Moreover, it is the first time to demonstrate that the pyroptosis executor GSDME is essential for HSC reconstitution, and we shed light on the interplay of apoptosis and GSDME-mediated pyroptosis in HSCs. Furthermore, we proved that GSDME is not the only mediator of HSC pyroptosis. Briefly, our study may help us to understand more about programmed death in HSCs as well as the role of GSDME in HSC maintenance.

Our study found that HSPCs underwent GSDME-dependent pyroptosis in response to the pro-apoptotic stimulus cisplatin (Fig. 4**A–F**). The choice of death forms for HSCs may be explained by the hypothesis we mentioned before.[21] In brief, pyroptosis is a form of necrotic cell death and may save more energy than apoptosis, thus pyroptosis may fit better for HSCs with a low metabolic state. This study will change the concept that HSCs undergo apoptosis upon Caspase-3 activation induced by apoptotic stimuli. Cisplatin has been reported to induce pyroptosis in GSDME expressing-cell lines.[24] It is the first time to prove that pyroptosis is able to happen in cisplatin-treated HSCs. However, GSDME is only responsible for partial cisplatin-induced necrotic cell death in HSPCs (Fig. 4**D–F**), which is similar to that in mouse macrophages.[28] Given the pyroptotic morphology in *Gsdme*-deficient HSPCs (Fig. 4**D**), we assume that other gasdermin family members may also involve in cisplatin-induced pyroptosis. This may be true since GSDME is not the only gasdermin involved in cell death after apoptosis induction,[16] for example Caspase-8 activation during TAK1 inhibition can activate both GSDME and GSDMD,[29] and Caspase-8 was reported to be activated by cisplatin.[30,31] Caspase-1 which can lead to GSDMD-dependent pyroptosis can be activated by cisplatin in mouse macrophages.[28] Moreover, GSDMA was reported to be upregulated in TGF-β induced apoptosis.[32] The roles of other gasdermin family members in HSCs are needed to be clarified in further studies. Furthermore, the energy may be not abundant for proliferative HSPCs and they would thus like to undergo necrotic cell death but not apoptosis even when *Gsdme* is deficient.

Our previous study demonstrated that overactive GSDME impaired the reconstitution capacity of HSCs,[21] while here, we demonstrate that *Gsdme* deletion impairs HSC function (Fig. 2**B, G**). The present result seems to be conflicted with our previous study, but it can be explained that a balanced cell death pathway is necessary for HSC maintenance. The increased apoptotic activity of cultured *Gsdme*$^{-/-}$ HSPCs indicates that GSDME connects apoptosis and pyroptosis in HSCs (Fig. 3**B,C**). Furthermore, the activation of Caspase-3 is enhanced in cultured *Gsdme*$^{-/-}$ HSPCs (Fig. 3**C,D**), which provides direct evidence that GSDME is essential to balance pyroptosis and apoptosis. Increased activity of Caspase-3 has also been reported in *Gsdmd*$^{-/-}$ bone marrow-derived macrophages (BMDMs) upon LPS plus nigericin treatment,[17] thus a similar mechanism may be shared by gasdermins to balance pyroptosis and apoptosis. Since GSDME is a substrate of Caspase-3,[24] we assume that the higher

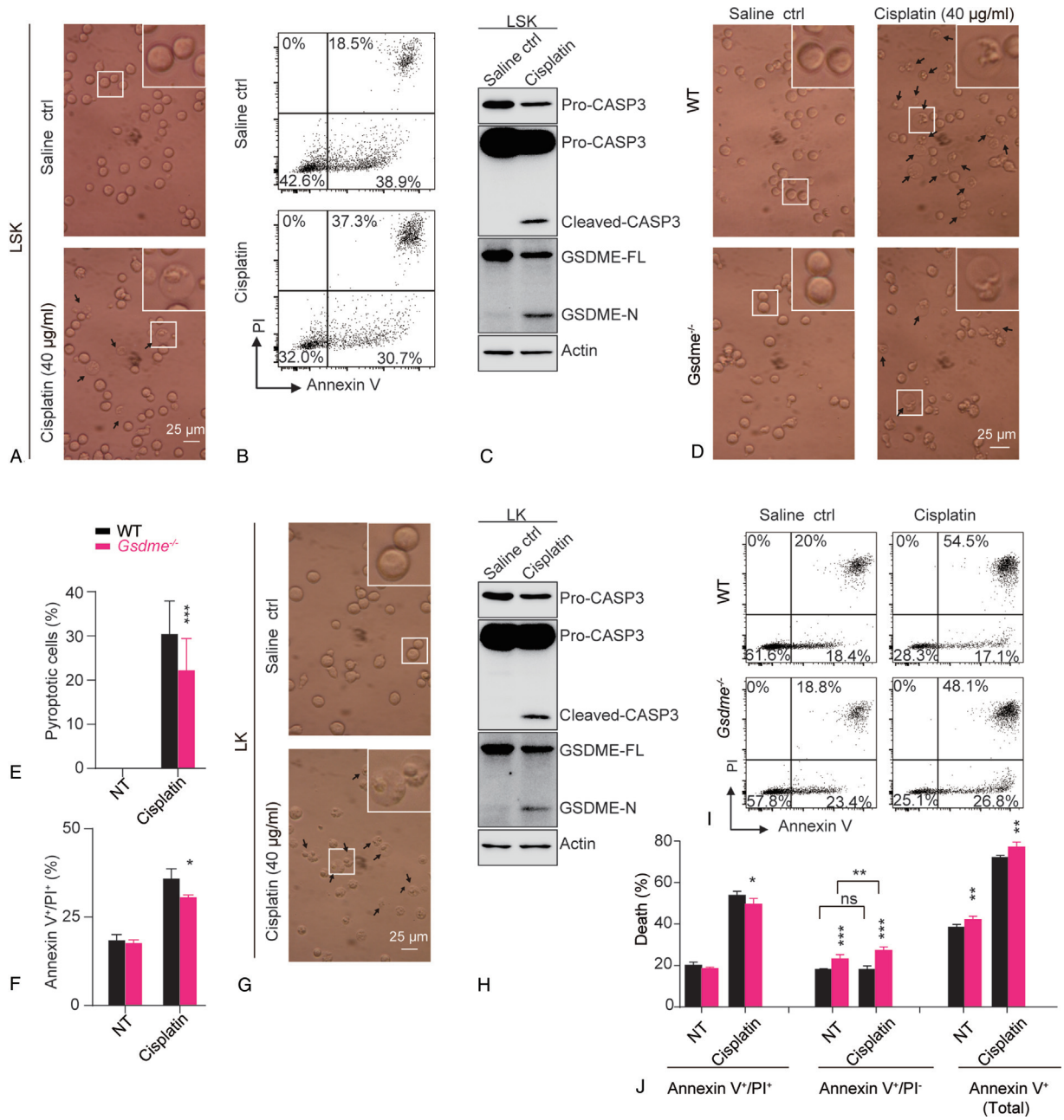

Figure 4. Cisplatin induces GSDME-dependent pyroptosis in HSPCs. (A, D, and G) The images show the pyroptotic morphology of cisplatin treated HSPCs. WT LSKs (A), LSKs from WT and *Gsdme*$^{-/-}$ mice (D), or WT LKs (G) were freshly isolated and treated with 40 μg/ml cisplatin for 6 h before the photos were taken. Pyroptotic cells are marked with black arrows. Scale bars, 25 μm. (B) Representative flow cytometry plots showing cell viability of cisplatin-treated LSKs. Freshly isolated LSKs were cultured overnight and subjected to 20 μg/ml cisplatin for 6.5 h before Annexin-V and PI staining. (C, H) Representative Western blot showing the activity of Caspase-3 and GSDME in cisplatin-treated LSKs (C) and LKs (H). Freshly isolated LSKs (C) or LKs (H) were cultured overnight and treated with 40 μg/ml cisplatin for 5 h before the Western blot assay. (E) The histogram shows the statistic result for the percentage of pyroptotic LSKs in (D). 488 WT LSKs and 581 *Gsdme*$^{-/-}$ LSKs were randomly analyzed. Data are shown as mean ± SD (F) The histogram depicts the frequency of Annexin-V$^+$/PI$^+$ cells of cisplatin-treated LSKs from WT and *Gsdme*$^{-/-}$ mice. Freshly isolated LSKs were cultured overnight and treated with 20 μg/ml cisplatin for 6.5 h before the cell viability assay by flow cytometry. n = 3 technical repeats per group, data are shown as mean ± SD. (I, J) Representative flow cytometry plots (I) and histograms (J) showing cell viability of cisplatin-treated LKs. Cisplatin were used at 20 μg/ml for 6.5 h. n = 4 technical repeats per group, data are shown as mean ± SD. (J-left) Annexin-V$^+$/PI$^+$; (J-middle) Annexin-V$^+$/PI$^-$; (J-right) Annexin-V$^+$.

apoptotic activity in *Gsdme*$^{-/-}$ HSPCs may be caused by a loss of competitive binding of GSDME with other substrates of Caspase-3 that can enhance apoptotic signals. For example, the C-terminus of BECN1 produced by the cleavage of caspases including Caspase-3 enhances apoptosis.[33]

However, *Gsdme* deficiency does not impair the homeostasis of the hematopoietic system at steady-state conditions (Fig. 1**A–G**), but it reduces HSC regeneration (Fig. 2**B,G**). Given that most HSCs are quiescent at steady-state conditions but proliferate during transplantation,[34] and that the cell viability of *Gsdme*-deficient HSPCs upon proliferation is reduced (Fig. 3**B**), we assume that the apoptosis signal may be elevated during HSC proliferation and may be even strengthened in *Gsdme*-deficient HSCs. A higher risk of apoptosis for proliferative HSCs may be true on account of the

increased DNA damage, which can be confirmed by the accumulation of γH2AX and DNA damage response in cycling HSCs.[35,36] Given that some inflammatory factors can drive HSC proliferation,[37] the inflammatory environment and danger-associated molecular patterns in the BM of irradiated recipients[37] may also be insults that lead to the death of *Gsdme*$^{-/-}$ HSCs. Similar to GSDME which works as a switch between pyroptosis and apoptosis, the apoptosis mediator Caspase-8 works as a switch between apoptosis and necroptosis,[12] the loss of function of Caspase-8 impairs the function of hematopoietic progenitors and causes monocytes death.[38] Collectively, different cell death pathways may be mutually restrained and the fine balance of them maintains HSC function.

However, since the necrotic cells are easily lost during HSC isolation, we could not provide direct evidence to prove whether GSDME-mediated pyroptosis mediated HSC death under physiological conditions, but the in vivo HSC transplantation experiments can provide evidence that GSDME functions during stress conditions. In summary, our study demonstrates that GSDME can mediate HSC pyroptosis upon apoptotic stimuli and that GSDME plays an essential role in HSC regeneration via the interplay of GSDME-mediated pyroptosis and apoptosis.

There are still lots of questions remaining to be settled. Further proofs should be provided to explain how GSDME functions to balance pyroptosis and apoptosis in HSCs. Moreover, the functions of other gsdermins in HSCs and how GSDME interplays with them, and the possible compensation genes of *Gsdme* in HSCs are worth studying in further investigations.

4. MATERIALS AND METHODS

4.1. Animals

Gsdme$^{-/-}$ (C57BL/6, CD45.2) mice[24] were a gift from Dr Feng Shao. C57BL/6-SJL (CD45.1) (Stock No: 002014) and C57BL/6 WT (CD45.2) (Stock No: 000664) mice were from the Jackson Laboratory. CD45.1/2 mice were heterozygotes from CD45.1 and CD45.2 mice. All the mice were maintained under the SPF conditions at Tsinghua University according to the protocols approved by the IACUC.

4.2. Complete blood cell and bone marrow cell count

PB was collected with an EDTA-containing tube from the tail and performed by the automatic hematology analyzer (BC-5000, Mindary). Single-cell suspension samples from BM were analyzed by Vi-CELL XR cell viability analyzer (Beckman Coulter).

4.3. Flow cytometry

Flow cytometry analysis and cell sorting were performed as previously described.[21] Briefly, bones from hindlimbs, pelvic bones (with spines for some experiments) were crushed and filtered for single-cell suspension. For HSC or LSK sorting, c-Kit$^+$ cells were enriched and stained with biotin-labeled lineage antibodies (biotin-lineage mix) followed by Streptavidin-APC-Cy7, Sca-1-PE-Cy7, c-Kit-APC for LSK and CD150-PE, CD34-FITC additional for HSC. For HSC and progenitor analysis, femurs-derived BM cells were stained with Streptavidin-APC-Cy7, Sca-1-PE-Cy7, c-Kit-APC, CD34-AF700, Flt3-PE-CF594, CD16/32-FITC, CD127-Brilliant Violet 421 following the biotin-lineage mix. For lineage analysis, femur-derived BM and PB samples were stained with CD3-APC, B220-PB, and CD11b-PerCP-Cy5.5. For lineage in recipient mice, CD45.1-FITC and CD45.2-PE were co-stained for HSC transplantation, and CD45.1-PE for RNAi experiment. Red blood cells in PB samples were lysed by ACK buffer before the antibodies staining. For HSPC chimerism analysis in recipients, BM cells were co-stained with CD45.1-FITC and CD45.2- PerCP-Cy5.5ith besides HSC markers. The detailed information for the antibodies used in flow cytometry was described previously.[21]

Cell sorting was performed on Influx/FACS Aria SORP (BD Biosciences), and hematopoietic analysis was performed on Fortessa (LSR Fortessa, BD Biosciences). 10ng/ml DAPI was used to indicate dead cells.

4.4. Transplantation

For HSC transplantation, 50 HSCs (CD34$^-$CD150$^+$LSK, CD45.2) were freshly isolated and transplanted with 5×10^5 complete BM cells (CD45.1) into lethally irradiated recipients (CD45.1/2). Lineage analysis for donor (CD45.2) chimerism was performed every month until the fourth month according to the antibodies listed above. HSPCs chimerism was analyzed at the end of the fourth month.

For RNAi transduced HSC transplantation, 10^5 LSKs isolated from hind limbs and spines of WT mice (CD45.2) were infected with lentivirus carrying the shRNA targeting the gene or the non-target control shRNA. 2.5×10^4 GFP$^+$ cells were isolated and co-transplanted with 3.125×10^5 competitors (CD45.1) into lethally irradiated recipients (CD45.2). Lineage analysis for GFP chimerism was performed every month until the third month according to the antibodies listed above.

4.5. In vitro cell culture and treatment

293T cells were maintained in DMEM supplied with 10% FBS and 50 U/ml penicillin/streptomycin (Hyclone, SV30010). LSKs were cultured in SFEM (Stem Cell Technologies, #09650, Vancouver, Canada) supplied with 50 U/ml penicillin/streptomycin, 20 ng/ml mTPO (Peprotech, 315-14), and 20 ng/ml mSCF (Peprotech, 250-03). For cisplatin treatment, LSKs were cultured overnight and treated with cisplatin (Harvey, HZB0054-100) or saline. 4 to 5×10^4 LSKs cultured in 96-well plated were treated with 40 μg/ml cisplatin for 6 hours for cell morphology assay, and 6000 to 8000 cells cultured in 96-well plated were treated with 20 μg/ml cisplatin for 6.5 for Annexin-V and PI staining. 2×10^5 LK cells were treated with 40 μg/ml cisplatin for 5 hours for Western blot assay (24 well plate). For lentivirus infection, 10^5 freshly isolated LSKs were plated in the well of 96-well plate with 100 μl SFEM, the virus was added to the cells 3 to 4 hours later, and cells were washed and transplanted to 24-well plated 11 to 12 hours post the lentivirus infection.

4.6. Cell viability and morphology assay

Cell viability assay was performed by Annexin-V and PI staining as previously described.[21] Cell morphology assay was performed by static bright-field images taken by a phase-contrast microscope (Olympus, CKX-41).

4.7. Western blot analysis and related antibodies

Cells were collected and sonicated by Sonicator (Diagenode, Bioruptor plus) in 1 × SDS loading (2% SDS, 25 mM Tris base/pH 6.8, 10% glycerol, 0.02% Bromphenolblau). Cell lysates were boiled at 100°C for 8 min and subjected to 13% SDS-PAGE with the antibody against Caspase-3 (1:800, CST, 9662S), and 10% SDS-PAGE with the antibody against GSDME (1:1000, Abcam, ab215191). Actin (1:1000, HuaBio, ET1701-80) and H3 (1:1000, Proteintech, 17168-1-AP) were used as the internal reference. All the original Western blot data were presented in (Sup. Fig. 3, http://links.lww.com/BS/A26).

4.8. Plasmid construction

The shRNA sequence (TGCTGTTGACAGTGAGCGCCCC-GACAAAATGTTTGCCAAATAGTGAAGCCACAGATGTAT-TTGGCAAACATTTTGTCGGGTTGCCTACTGCCTCGGA) targeting GSDME was cloned into SF-LV-miRE-EGFP plasmid.

4.9. Lentivirus production and concentration

Lentivirus was packaged and concentrated as previously described.[21] Briefly, the shRNAs and helper plasmids were transfected to 293T cells using Polyethylenimine (Polysciences, 23966). Supernatants were collected at 48- and 72-hours post transfection and then concentrated (250×) by ultracentrifuge (Beckman, OPTIMA XE-90).

4.10. Statistics

GraphPad Prism 6.0 was used for statistical analyses. *P* values were calculated by 2-tailed Student's *t* test (unpaired). Significance: $*P \leq .05$, $**P \leq .01$, $***P \leq .001$. All experiments were repeated independently at least twice.

ACKNOWLEDGMENTS

This work was supported by grant numbers 2018YFA0800200, 2017YFA0104000, Z181100001818005 to J.W.W. from the National Key R&D Program of China or the Beijing Municipal Science & Technology Commission.
We thank Dr Feng Shao for the gift of *Gsdme*$^{-/-}$ mice.

REFERENCES

[1] Domen J, Cheshier SH, Weissman IL. The role of apoptosis in the regulation of hematopoietic stem cells: overexpression of Bcl-2 increases both their number and repopulation potential. *J Exp Med* 2000;191 (2):253–264.
[2] Yu H, Shen H, Yuan Y, et al. Deletion of Puma protects hematopoietic stem cells and confers long-term survival in response to high-dose γ-irradiation. *Blood* 2010;115 (17):3472–3480.
[3] Wang J, Lu X, Sakk V, Klein CA, Rudolph KL. Senescence and apoptosis block hematopoietic activation of quiescent hematopoietic stem cells with short telomeres. *Blood* 2014;124 (22):3237–3240.
[4] Yamashita M, Passegue E. TNF-alpha coordinates hematopoietic stem cell survival and myeloid regeneration. *Cell Stem Cell* 2019;25 (3):357–372.e7.
[5] Masters Seth L, Gerlic M, Metcalf D, et al. NLRP1 inflammasome activation induces pyroptosis of hematopoietic progenitor cells. *Immunity* 2012;37 (6):1009–1023.
[6] Zhang Y, Chen X, Gueydan C, Han J. Plasma membrane changes during programmed cell deaths. *Cell Res* 2018;28 (1):9–21.
[7] Frank D, Vince JE. Pyroptosis versus necroptosis: similarities, differences, and crosstalk. *Cell Death Differ* 2019;26 (1):99–114.
[8] Jorgensen I, Rayamajhi M, Miao EA. Programmed cell death as a defence against infection. *Nat Rev Immunol* 2017;17 (3):151–164.
[9] Domen J, Gandy KL, Weissman IL. Systemic overexpression of BCL-2 in the hematopoietic system protects transgenic mice from the consequences of lethal irradiation. *Blood* 1998;91 (7):2272–2282.
[10] Chang J, Wang Y, Shao L, et al. Clearance of senescent cells by ABT263 rejuvenates aged hematopoietic stem cells in mice. *Nat Med* 2015;22 (1):78–83.
[11] Wang H, Sun L, Su L, et al. Mixed lineage kinase domain-like protein MLKL causes necrotic membrane disruption upon phosphorylation by RIP3. *Mol Cell* 2014;54 (1):133–146.
[12] Yuan J, Najafov A, Py BF. Roles of caspases in necrotic cell death. *Cell* 2016;167 (7):1693–1704.
[13] Rickard JA, O'Donnell JA, Evans JM, et al. RIPK1 regulates RIPK3-MLKL-driven systemic inflammation and emergency hematopoiesis. *Cell* 2014;157 (5):1175–1188.
[14] Janzen V, Fleming HE, Riedt T, et al. Hematopoietic stem cell responsiveness to exogenous signals is limited by caspase-3. *Cell Stem Cell* 2008;2 (6):584–594.
[15] Maryanovich M, Oberkovitz G, Niv H, et al. The ATM-BID pathway regulates quiescence and survival of haematopoietic stem cells. *Nat Cell Biol* 2012;14 (5):535–541.
[16] Broz P, Pelegrin P, Shao F. The gasdermins, a protein family executing cell death and inflammation. *Nat Rev Immunol* 2020;20 (3):143–157.
[17] He WT, Wan H, Hu L, et al. Gasdermin D is an executor of pyroptosis and required for interleukin-1beta secretion. *Cell Res* 2015;25 (12):1285–1298.
[18] Fink SL, Cookson BT. Caspase-1-dependent pore formation during pyroptosis leads to osmotic lysis of infected host macrophages. *Cell Microbiol* 2006;8 (11):1812–1825.
[19] Liu YG, Chen JK, Zhang ZT, et al. NLRP3 inflammasome activation mediates radiation-induced pyroptosis in bone marrow-derived macrophages. *Cell Death Dis* 2017;8 (2):e2579.
[20] Shi J, Zhao Y, Wang K, et al. Cleavage of GSDMD by inflammatory caspases determines pyroptotic cell death. *Nature* 2015;526 (7575): 660–665.
[21] Yang X, Ge L, Wang J. BECN1 modulates hematopoietic stem cells by targeting Caspase-3-GSDME-mediated pyroptosis. *Blood Sci* 2020;2 (3):89–99.
[22] Wilkinson MF. Genetic paradox explained by nonsense. *Nature* 2019;668 (2019):179–180.
[23] Morrison SJ, Wandycz AM, Akashi K, Globerson A, Weissman IL. The aging of hematopoietic stem cells. *Nat Med* 1996;2 (9):1011–1016.
[24] Wang Y, Gao W, Shi X, et al. Chemotherapy drugs induce pyroptosis through caspase-3 cleavage of a gasdermin. *Nature* 2017;547 (7661): 99–103.
[25] Crowley LC, Marfell BJ, Scott AP, Waterhouse NJ. Quantitation of apoptosis and necrosis by Annexin V binding, propidium iodide uptake, and flow cytometry. *Cold Spring Harb Protoc* 2016;2016 (11):953–957.
[26] Vande Walle L, Lamkanfi M. Pyroptosis. *Curr Biol* 2016;26 (13):R568–R572.
[27] Galluzzi L, Senovilla L, Vitale I, et al. Molecular mechanisms of cisplatin resistance. *Oncogene* 2012;31 (15):1869–1883.
[28] Mai FY, He P, Ye JZ, et al. Caspase-3-mediated GSDME activation contributes to cisplatin- and doxorubicin-induced secondary necrosis in mouse macrophages. *Cell Prolif* 2019;52 (5): (e12663):
[29] Sarhan J, Liu BC, Muendlein HI, et al. Caspase-8 induces cleavage of gasdermin D to elicit pyroptosis during Yersinia infection. *Proc Natl Acad Sci USA* 2018;115 (46):E10888–E10897.
[30] Liu J, Uematsu H, Tsuchida N, Ikeda M-A. Association of caspase-8 mutation with chemoresistance to cisplatin in HOC313 head and neck squamous cell carcinoma cells. *Biochem Biophys Res Commun* 2009;390 (3):989–994.
[31] Seki K, Yoshikawa H, Shiiki K, Hamada Y, Akamatsu N, Tasaka K. Cisplatin (CDDP) specifically induces apoptosis via sequential activation of caspase-8, -3 and -6 in osteosarcoma. *Cancer Chemother Pharmacol* 2000;45 (3):199–206.
[32] Saeki N, Kim DH, Usui T, et al. GASDERMIN, suppressed frequently in gastric cancer, is a target of LMO1 in TGF-beta-dependent apoptotic signalling. *Oncogene* 2007;26 (45):6488–6498.
[33] Wirawan E, Vande Walle L, Kersse K, et al. Caspase-mediated cleavage of Beclin-1 inactivates Beclin-1-induced autophagy and enhances apoptosis by promoting the release of proapoptotic factors from mitochondria. *Cell Death Dis* 2010;1 (1):e18.
[34] Wilson A, Laurenti E, Oser G, et al. Hematopoietic stem cells reversibly switch from dormancy to self-renewal during homeostasis and repair. *Cell* 2008;135 (6):1118–1129.
[35] Flach J, Bakker ST, Mohrin M, et al. Replication stress is a potent driver of functional decline in ageing haematopoietic stem cells. *Nature* 2014;512 (7513):198–202.
[36] Beerman I, Seita J, Inlay MA, Weissman IL, Rossi DJ. Quiescent hematopoietic stem cells accumulate DNA damage during aging that is repaired upon entry into cell cycle. *Cell Stem Cell* 2014;15 (1):37–50.
[37] Schuettpelz LG, Link DC. Regulation of hematopoietic stem cell activity by inflammation. *Front Immunol* 2013;4:204.
[38] Kang TB, Ben-Moshe T, Varfolomeev EE, et al. Caspase-8 serves both apoptotic and nonapoptotic roles. *J Immunol* 2004;173 (5):2976–2984.